International Scholarly Research Network
ISRN Renewable Energy
Volume 2011, Article ID 651857, 6 pages
doi:10.5402/2011/651857

Research Article

A Study of the Hazardous Glare Potential to Aviators from Utility-Scale Flat-Plate Photovoltaic Systems

Evan Riley and Scott Olson

Black & Veatch Corporation, Energy Division, 650 California Street, Fifth Floor, San Francisco, CA 94108, USA

Correspondence should be addressed to Evan Riley, rileye@bv.com

Received 15 August 2011; Accepted 17 September 2011

Academic Editors: E. R. Bandala, S. Dai, S. S. Kalligeros, and A. Stoppato

The potential flash glare a pilot could experience from a proposed 25-degree fixed-tilt flat-plate polycrystalline PV system located outside of Las Vegas, Nevada, was modeled for the purpose of hazard quantification. Hourly insolation data measured via satellite for the years 1998 to 2004 was used to perform the modeling. The theoretical glare was estimated using published ocular safety metrics which quantify the potential for a postflash glare after-image. This was then compared to the postflash glare after-image potential caused by smooth water. The results show that the potential for hazardous glare from flat-plate PV systems is similar to that of smooth water and not expected to be a hazard to air navigation.

1. Introduction

Before construction of utility scale photovoltaic (PV) power plants near airports or within known flight corridors in the United States, the Federal Aviation Administration (FAA) requires that the glare from the proposed plant not be a hazard to navigable airspace [1]. The purpose of this paper is to demonstrate that glare from flat-plate PV power plants is similar to that of water and therefore does not pose a hazard to navigable airspace.

This was done by calculating the glare potential from a theoretical flat-plate PV power plant located near Las Vegas, Nevada, and comparing that glare to the glare potential of smooth water.

To estimate potential glare from flat surfaces, a model developed which used conservative assumptions. This model is a generalization of work done by Ho et al. [1]. The model calculated glare hourly from 1998 to 2004 to find the times when the possibility for glare would be the greatest. The potential for after-image (hazardous glare) was then compared to the potential for hazardous glare from smooth water which pilots often view while on approach to land.

2. Method

A review of published literature on modeling glare was conducted. The effects of glare on humans has been quantified by Metcalf and Horn [2], Saur and Dobrash [3], Severin et al. [4], and Sliney and Freasier [5]. In other studies Brumleve [6], Chiabrando et al. [7], and Ho et al. [1] developed mathematical methods to quantify the potential danger of glare causing flash blindness. Flash blindness is defined by Ho as a "temporary disability or distraction" that can cause an after-image and is understood to be comparable to what a human experiences when viewing the flash of a camera.

Ho explains in detail various methods for modeling glare from concentrating solar systems which use mirrors and lenses to concentrate light onto a central receiver. This technology is different than flat-plate PV modules which directly convert solar energy to electricity. However, the after-image estimation method Ho outlines for concentrating solar systems is easily generalized to flat-plate PV modules. The flow diagram in Figure 1 shows the general method implemented to translate solar radiation to the after-image potential caused by energy received on an observer's retina.

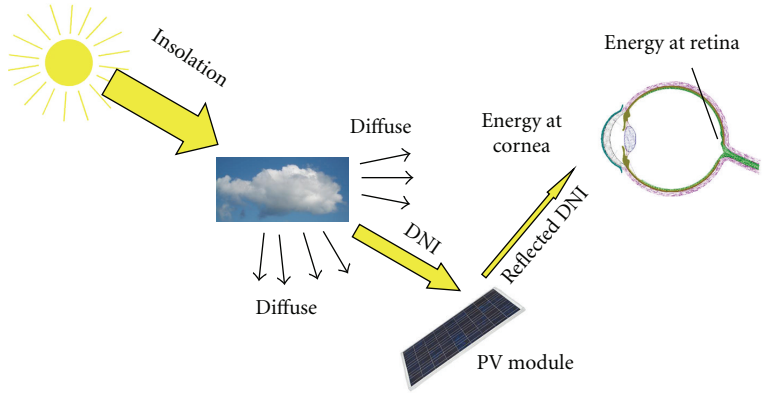

Figure 1: Energy flow diagram.

The subsections below provide more detail for each step of the process.

2.1. Insolation. The SUNY-Perez Satellite dataset was used for modeling glare. The National Renewable Energy Laboratory (NREL) compiled this dataset for the years 1998 to 2005 on an hourly basis for a 10×10 km nationwide grid.

Solar radiation in the visible spectrum can be broken up into two primary components, diffuse and direct. Diffuse radiation is defined as radiation that has been scattered by the atmosphere. Direct radiation, also commonly referred to as beam, is radiation which moves from the source to the observer via the shortest distance possible without scattering. For example, on a heavily overcast day when the sun is highest in the sky (solar noon), it is probable that all insolation is diffuse. On a clear day at solar noon, most of the insolation reaching earth's surface would be direct. Direct radiation is the component of solar radiation that causes visible glare from flat plate PV systems.

2.2. PV Module. The next step in the modeling process was to quantify the amount of visible radiation would be reflected off of a PV module for every hour from 1998 to 2004. The year 2005 was omitted for computational reasons. This was done by multiplying the power (Watts per square centimeter, or W/cm^2) of direct radiation with the reflectivity of the PV module at the average incidence angle for each hour evaluated.

Incidence angle is defined as the angle between the direct component of insolation and a ray perpendicular to the module. If the incidence angle is zero, the angle between the surface of the module and the direct component of radiation is 90°. The reflectance at 633 nm of a polycrystalline silicon (p-Si) PV module is a function of the incidence angle as seen below in Figure 2 developed by Parretta et al. [8]. This reflectance as a function of incidence angle was to determine how much of the direct insolation in the visible spectrum would be reflected off of the PV module and thus reach the observer.

The data shown above is for a glass encapsulated p-Si solar cell. The use of this data is a conservative assumption as the glass used to encapsulate the cell was not solar glass and no antireflective coating applied to the p-Si cell. Actual p-Si modules would likely have lower reflectance values as textured glass, and antireflective coatings are often used to reduce reflected irradiance and increase module efficiency.

The power of the reflected direct radiation was calculated hourly from 1998 to 2004 using the reflectivity in Figure 2, satellite data from NREL, and established sun position equations. The use of hourly data allows quantification of how the power of the reflected direct radiation will vary as the sun moves across the sky.

2.3. Energy at the Cornea. An assumption was made that the power of the direct radiation reflected off of the PV module was equal to the power incident on the cornea of the pilot. This is a conservative assumption as it ignores atmospheric attenuation, refraction, and further reflection. While it is likely that there will be energy diffusion or absorption due to the atmosphere, cockpit glass, or shielding, these effects were ignored during this initial estimation. Later calculations took these potential mitigation efforts into account, as can be seen in Figure 7.

2.4. Retinal Irradiance. The last step in the modeling process was to calculate retinal irradiance hourly from 1998 to 2004. Retinal irradiance can be calculated us a derivation provided by Sliney [9] from the energy incident on the cornea as

$$E_r = E_c \left(\frac{d_p}{f\omega} \right)^2 \tau, \tag{1}$$

where E_r is retinal irradiance [W/cm^2], E_c is irradiance at a plane in front of the cornea [W/cm^2], f is the focal length of the eye (~0.17 cm), d_p is the diameter of the human pupil adjusted to sunlight (~0.2 cm), ω is the subtended angle of the image (or apparent size of the image which in the case of the sun is 0.0093 radians), and τ is the transmission coefficient of the eye (~0.5). This equation assumes that the arc of a circle f is equal to its chord, which is a good approximation for small angles such as these.

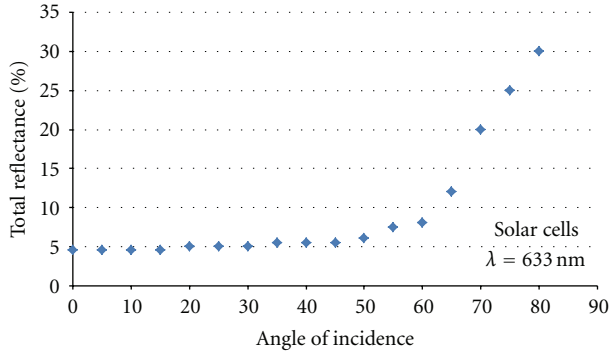

Figure 2: Reflectance as a Function of Incident Angle [8].

3. Ocular Safety Metrics

Next, the calculated values of retinal irradiances were compared to known ocular safety metrics. Extensive research has been done on ocular safety metrics and how to calculate the potential for after-image or retinal burns from radiation in the visible wavelengths. The threshold for retinal irradiance corresponding to the potential for retinal burns has been defined as

$$E_{r,\text{burn}} = \frac{0.118}{\omega} \quad \text{for } \omega < 0.118,$$
$$E_{r,\text{burn}} = 1 \quad \text{for } \omega \geq 0.118, \tag{2}$$

where $E_{r,\text{burn}}$ is the retinal burn threshold [W/m^2] and ω is the subtended angle of the sun or 0.0093 radians, Ho et al. [1], and Sliney and Freasier [5]. Ho also compiled data from Metcalf and Horn [2], Severin et al. [4], and Saur and Dobrash [3] to find a fit corresponding to the minimal retinal irradiances that caused after-image (glare). This is calculated by

$$E_{r,\text{flash}} = \frac{3.59 \times 10^{-5}}{\omega^{1.77}}, \tag{3}$$

where $E_{r,\text{flash}}$ is the threshold for potential after image [W/cm^2]. Ho then plotted both of these thresholds and the three regions these thresholds define (potential for retinal burn, potential for after-image, and low potential for after-image) which are illustrated in Figure 3.

The subtended source angle is a function of the size of the image viewed. For the purposes of this report, the image is a reflection of the sun which causes the subtended angle to be constant at 0.0093 radians or roughly 10 mrads.

4. Results

Retinal irradiance was calculated hourly from the years 1998 to 2004 for a fixed-tilt polycrystalline system under the assumptions illustrated in Table 1. These results were then compared to the same results from smooth water.

The assumption of a fixed-tilt system is conservative because, as seen in Figure 2, the reflected component of irradiances increases as incidence angle increases. Having the system held at a fixed tilt increases the average incident angle and therefore the average reflected irradiance.

Table 1: Retinal irradiance assumptions.

Module type	Polycrystalline silicon (p-Si)
Module Tilt/Azimuth	25°/0°
Atmospheric attenuation between the module and the pilot's eye?	No
Subtended angle of the sun	0.00093 radians
Diameter of the pupil in sunlight	0.2 cm
Focal length of the eye	0.0017 cm
Transmission coefficient of the eye	0.5

Table 2: Retinal irradiances.

	Median* [W/cm^2]	Maximum [W/cm^2]
Fixed-tilt p-Si	0.23	0.45
Smooth water	0.13	0.38
Low potential for an after-image <0.10 W/cm^2		
Potential for after-image = 0.10 to 12.7 W/cm^2		
Potential for retinal burn ≥12.7 W/cm^2		

*The median is calculated as the median of all hours with direct insolation greater than 0.

The results of the calculations are displayed in Figure 4 and Table 2. Figure 4 shows retinal irradiances for all hours in the six-year period when direct radiation was present. For example, the blue bar furthest to the left in Figure 4 represents the number of hours in the years 1998 to 2004 where retinal irradiance was between 0 and 0.02 W/cm^2 (approximately 2250 hours). The potential for an after-image corresponding to the different retinal irradiance powers are shown based on the zones defined in Figure 3. The ranges of these zones are quantified in Table 2, showing that a potential for an after-image for both PV panels and smooth water exists but is slight.

Table 2 shows that the median values of both distributions reside in the region "potential for an after-image." The histogram in Figure 4 shows that 79 to 88 percent of hourly retinal irradiances from smooth water and fixed PV modules fall in this region. However, all calculated retinal irradiances fall in the bottom 5% of the region, indicating that although

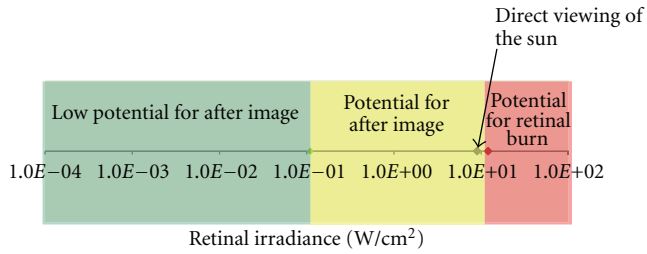

Figure 3: Potential impacts of retinal irradiance for a 0.15 s exposure from Ho et al. [1].

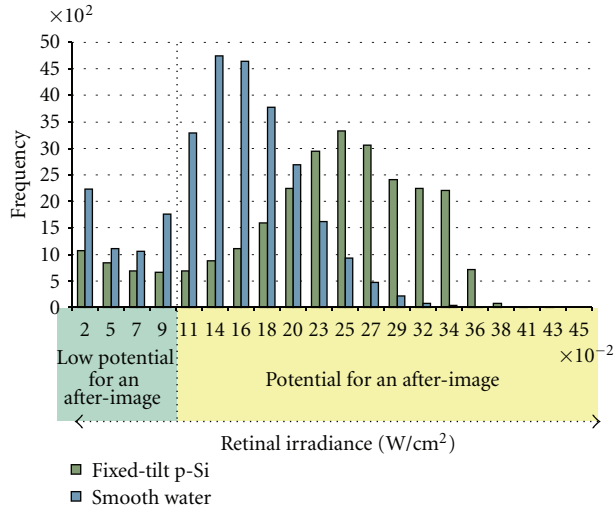

Figure 4: Frequency distribution of retinal irradiance 1998 to 2004.

the glare hazard exists, it is relatively low. Figure 5 illustrates this point by expanding the *x*-axis to the entire range of retinal irradiances that would be classified as "potential for an after-image." The major difference between this figure and the one developed by Ho in Figure 3 is the use of a linear, not logarithmic scale.

Figure 6 displays the *maximum* value of hourly glare (highest retinal irradiance) from smooth water and fixed tilt p-Si PV modules plotted onto Figure 3.

As can be seen from Figure 6, the maximum glare from a solar PV array using conservative assumptions is expected to be comparable to that of smooth water. This maximum value is in the region defined as "potential for after-image" where a potential exists, but the potential is on the low end of the range.

The nuisance of glare for pilots cannot be completely avoided. Therefore, it is typically mitigated using darkened visors, sunglasses, and glare shields. If these objects are manufactured to meet American National Standards Institute (ANSI) Standard Z80.3-2001 [10], they will reduce the intensity of retinal irradiance by roughly 70 percent. A 70 percent reduction of retinal irradiances from radiation reflected off of water and PV modules move all retinal irradiance values below 0.14 W/cm^2 as displayed below in Figure 7. Under these conditions, 92 percent of the hours over the six-year period investigated for solar PV would now be in the "low potential" zone in Las Vegas.

5. Conclusions

The potential flash glare a pilot could experience was modeled from a proposed 25-degree fixed-tilt flat-plate polycrystalline PV array installed outside of Las Vegas, Nevada. Hourly insolation data measured onsite via satellite from the years 1998 to 2004 was used to perform this modeling. These results were then compared to the potential glare from smooth water under the same assumptions. The comparison of the results showed that the potential for glare from flat plate PV systems is comparable to that of smooth water and not expected to be a hazard to air navigation.

Glare from ground-based objects can be a nuisance to pilots if proper mitigation procedures are not implemented. Portland white cement concrete (which is a common concrete for runways), snow, and structural glass all have reflectivities greater than water and flat plate PV modules as shown by Levinson and Akbari [11], Nakamura etal. [12] and Hutchins et al. [13]. Pilots viewing these objects under specific conditions may experience a distracting level of glare.

The nuisance of glare cannot be completely avoided. Therefore, it is typically mitigated using darkened visors, sunglasses, and glare shields. If these objects are manufactured to meet ANSI Standard Z80.3-2001 [10], they will reduce the intensity of retinal irradiance by roughly 70 percent. A 70-percent reduction of retinal irradiances from radiation reflected off of water and PV modules move all retinal

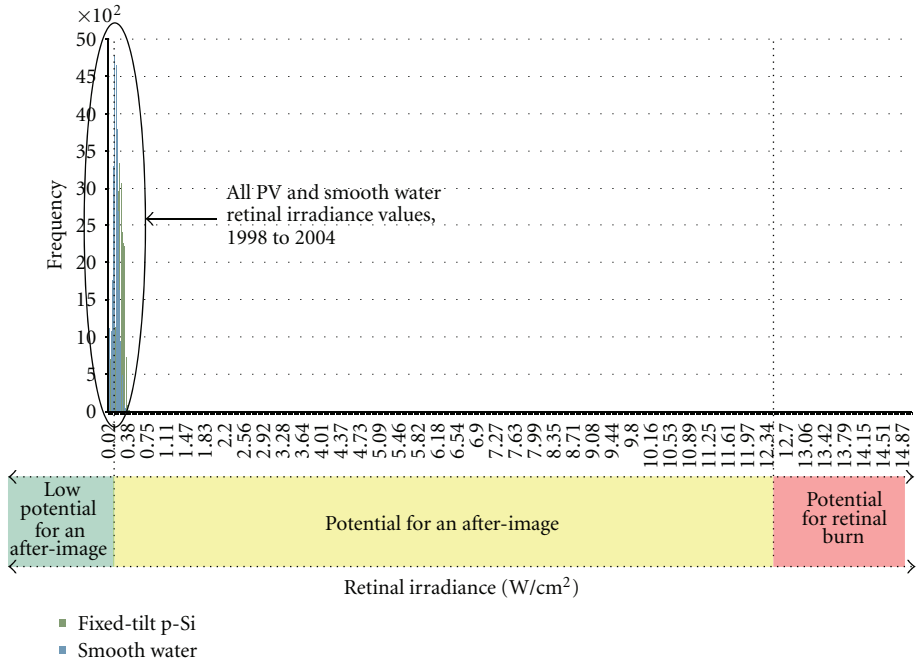

Figure 5: Linearly scaled frequency distribution of retinal irradiance.

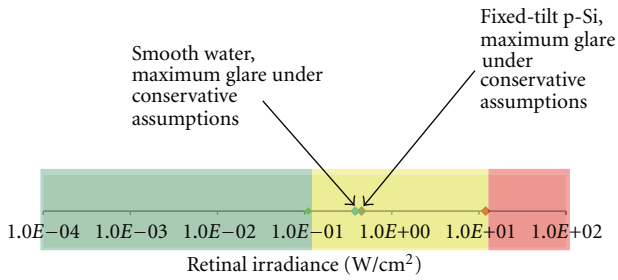

Figure 6: Calculated maximum glare at Nellis [1].

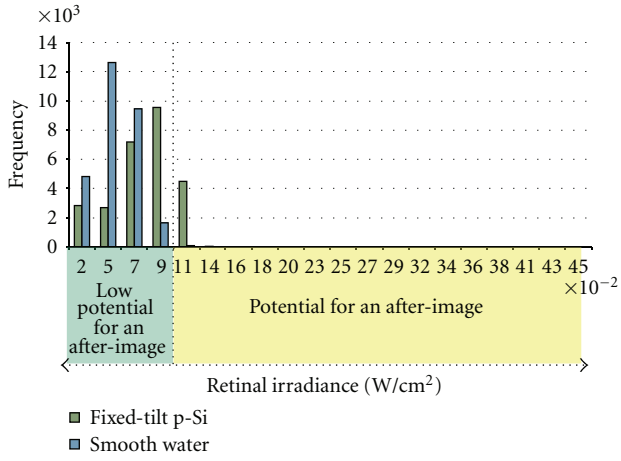

Figure 7: Frequency distribution of retinal irradiance with mitigation.

irradiance values below 0.14 W/cm^2. Under these conditions, 92 percent of the hours over the six-year period investigated for solar PV would now be in the "low potential" zone at Las Vegas.

Highlights

(i) Ocular safety metrics were used to quantify the potential for hazardous glare from a photovoltaic system hourly.

(ii) The results show that the glare hazard from smooth water and flat plate photovoltaic systems are similar.

(iii) Glare mitigation is common and significantly reduces glare hazards.

Abbreviations

ANSI: American National Standards Institute
NREL: National Renewable Energy Labs
PV: Photovoltaic
p-Si: Polycrystalline silicon.

Acknowledgments

Special thanks to NV Energy, Inc. specifically David Sims for sponsoring this work, and to Clifford K. Ho, Cheryl M. Ghanbari, and Richard B. Driver for deriving the optical equations applied in this research and for compiling the history of optical safety metrics into a single paper.

References

[1] C. Ho et al., "Methodology to assess potential glint and glare hazards from concentrating solar power plants: analytical models and experimental validation. s.l.," ES2010-90054, Sandia National Laboratories, 2010.

[2] R. D. Metcalf and R. E. Horn, "Visual recovery times from high intensity flashes of light. s.l.," Wright Air development Center Technical Report 58232, Air Force Aerospace Medical Research Lab, 1958.

[3] R. L. Saur and S. M. Dobrash, "Duration of after-image disability and viewing simulated sun reflections," *Applied Optics*, vol. 8, no. 9, pp. 1799–1801, 1969.

[4] S. L. Severin, N. L. Newton, and J. F. Culver, "An experimental approach to flash blindness," *Aeromedica acta*, vol. 33, pp. 1199–1205, 1962.

[5] D. H. Sliney and B. C. Freasier, "Evaluation of optical radiation hazards," *Applied Optics*, vol. 12, no. 1, pp. 1–24, 1973.

[6] T. D. Brumleve, "Eye hazard and glint evaluation for the 5-MWt solar thermal test facility," SAND76-8022, Sandia National Laboratories, Livermore, Calif, USA, 1977.

[7] R. Chiabrando, E. Fabrizio, and G. Garnero, "The territorial and landscape impacts of photovoltaic systems: definition of impacts and assessment of the glare risk," *Renewable and Sustainable Energy Reviews*, vol. 13, no. 9, pp. 2441–2451, 2009.

[8] A. Parretta, A. Sarno, P. Tortora et al., "Angle-dependent reflectance measurements on photovoltaic materials and solar cells," *Optics Communications*, vol. 172, no. 1, pp. 139–151, 1999.

[9] D. H. Sliney, "An evaluation of the potential hazards of the point focusing solar concentrators at the JPL-Edwards test site," JPL Consulting Agreement no. JF 714696, California Institute of Technology, Pasadena, Calif, USA, 1980.

[10] ANSI, "Ophthalmics—nonprescription sunglasses and fashion eyewear—requirements," ANSI Z80.3-2001. s.l., American National Standards Institute, 2001.

[11] R. Levinson and H. Akbari, "Effects and composition and exposure on the solar reflectance of portland cement concrete," LBL-48334, Lawerence Berkley National Laboratory, Berkley, Calif, USA, 2001.

[12] T. Nakamura, O. Abe, T. Hasegawa, R. Tamura, and T. Ohta, "Spectral reflectance of snow with a known grain-size distribution in successive metamorphism," *Cold Regions Science and Technology*, vol. 32, no. 1, pp. 13–26, 2001.

[13] M. G. Hutchins, A. J. Topping, C. Anderson et al., "Measurement and prediction of angle-dependent optical properties of coated glass products: results of an inter-laboratory comparison of spectral transmittance and reflectance," *Thin Solid Films*, vol. 392, no. 2, pp. 269–275, 2001.